HHS Public Access

Author manuscript

J Mol Histol. Author manuscript; available in PMC 2020 December 01.

Published in final edited form as:

J Mol Histol. 2019 December ; 50(6): 581–591. doi:10.1007/s10735-019-09851-x.

FAM20A is Essential for Amelogenesis, but is Dispensable for Dentinogenesis

Lili Li[§], **Wuliji Saiyin**[§], **Hua Zhang**, **Suzhen Wang**, **Qian Xu**, **Chunlin Qin**, **Yongbo Lu**[*]

Department of Biomedical Sciences and Center for Craniofacial Research and Diagnosis, Texas A&M University College of Dentistry, Dallas, TX 75246, USA

Abstract

Mutations in the gene encoding family with sequence similarity 20, member A (FAM20A) caused amelogenesis imperfecta (AI), in humans. However, the roles of FAM20A in amelogenesis and dentinogenesis are poorly understood. In this study, we generated a *Fam20a* knockout (*Sox2-Cre;Fam20a*$^{fl/fl}$) mouse model by crossing *Fam20a*$^{fl/fl}$ mice with *Sox2-Cre* transgenic mice, in which *Fam20a* was ablated in both dental epithelium and dental mesenchyme. We found that these mice developed an enamel phenotype that resembles human AI associated with FAM20A mutations, but did not have apparent dentin defects. The secretory stage ameloblasts in the mandibular incisors from the *Sox2-Cre;Fam20a*$^{fl/fl}$ mice were shorter and detached from the enamel matrix, and subsequently lost their polarity, became disorganized and formed numerous spherical extracellular matrices in place of normal enamel. At the molecular level, the *Sox2-Cre;Fam20a*$^{fl/fl}$ mice displayed dramatically reduced expression levels of the genes encoding the enamel matrix proteins, but unaltered levels of the genes encoding the dentin matrix proteins. Moreover, *Fam20a* ablation resulted in a great decrease in FAM20C protein level, but it did not alter the intracellular localization of FAM20C protein in ameloblasts and odontoblasts. These results indicate that FAM20A is essential for amelogenesis, but is dispensable for dentinogenesis.

Keywords

tooth development; enamel; dentin; biomineralization; cell differentiation; genetics

INTRODUCTION

Family with sequence similarity 20 (FAM20) consists of three members: A (FAM20A), B (FAM20B) and C (FAM20C). FAM20B is a kinase that phosphorylates the xylose residue in the glycosaminoglycan-protein linkage region (Koike et al. 2009). FAM20C is a Golgi-

[*]**To whom correspondence should be addressed:** Yongbo Lu, Department of Biomedical Sciences and Center for Craniofacial Research and Diagnosis, Texas A&M University College of Dentistry, 3302 Gaston Ave. Room 436, Dallas, TX 75246, USA, Phone: (+1)-214-828-8277; Fax: (+1)-214-874-4538; ylu@tamu.edu.

[§]Both authors contributed equally to this work.

localized casein kinase responsible for phosphorylating many luminal and secreted proteins, including proteins involved in biomineralization (Ishikawa et al. 2012; Tagliabracci et al. 2012; Tagliabracci et al. 2015). *FAM20C* mutations in humans result in Raine syndrome (Simpson et al. 2007; Simpson et al. 2009). FAM20A is believed to be a pseudokinase and does not have kinase activity itself, but it can form a complex with FAM20C and enhance FAM20C's kinase activity to phosphorylate secreted proteins within the secretory pathway (Cui et al. 2015). Mutations in *FAM20A* in humans cause autosomal recessive amelogenesis imperfecta and gingival fibromatosis syndrome (AIGFS; OMIM #614253) (O'Sullivan et al. 2011) or enamel renal syndrome (ERS; OMIM #204690) (Jaureguiberry et al. 2012; Wang et al. 2013a) or enamel-renal-gingival syndrome (Kantaputra et al. 2014). All of the inheritable diseases associated with *FAM20A* mutations invariably manifest enamel defects, known as hypoplastic amelogenesis imperfect (AI).

During tooth development, *Fam20a* and *Fam20c* are both expressed in ameloblasts and odontoblast (Li et al. 2016; Wang et al. 2014; Wang et al. 2010). Conditional deletion of *Fam20a* in the dental epithelium in mice resulted in a tooth phenotype that is similar to human hypoplastic AI associated with *FAM20A* mutations; in these mice, the ameloblasts in the mandibular molars were poorly differentiated, and detached from the enamel matrix, resulting in the formation of cystic lesions within the abnormal enamel organ (Li et al. 2016). A similar enamel phenotype has been observed in *Fam20a*-null mice (Vogel et al. 2012) as well as in *Fam20c*-deficient mice (Wang et al. 2013c; Wang et al. 2012b). Although FAM20A stimulates the kinase activity of FAM20C in phosphorylating enamel matrix proteins *in vitro* (Cui et al. 2015), the roles of FAM20A in ameloblasts and odontoblasts *in vivo* are largely unknown.

In this study, we generated a *Fam20a* knockout (*Sox2-Cre;Fam20a*$^{fl/fl}$) mouse model by crossing *Fam20a*$^{fl/fl}$ mice with *Sox2-Cre* transgenic mice, so that *Fam20a* was inactivated in both dental epithelium and dental mesenchyme. We found that these mice developed a human AI-like enamel phenotype, but did not have apparent dentin defects. Moreover, the *Sox2-Cre;Fam20a*$^{fl/fl}$ mice displayed dramatically reduced expression levels of the genes encoding the enamel matrix proteins, including amelogenin (*Amel*), ameloblastin (*Ambn*), enamelin (*Enam*) and amelotin (*Amtn*), but unaltered levels of the genes encoding the dentin matrix proteins, including dentin matrix protein 1 (*Dmp1*) and dentin sialophosphoprotein (*Dspp*). In addition, although *Fam20a* deletion caused a great decrease in FAM20C protein levels, it did not alter the intracellular localization of FAM20C protein in ameloblasts and odontoblasts. These findings indicate that FAM20A is essential for amelogenesis, but is dispensable for dentinogenesis.

MATERIALS &METHODS

Generation of *Sox2-Cre;Fam20a*$^{fl/fl}$ Mice

The *Sox2-Cre;Fam20a*$^{fl/fl}$ mice were generated by breeding *Fam20a*$^{fl/fl}$ (Li et al. 2016) with *Sox2-Cre* transgenic mice (the Jackson Laboratory). The Sox2-Cre transgene is active in epiblasts at embryonic day 6.5 (Hayashi et al. 2002); therefore, *Fam20a* is inactivated in nearly all the tissues and cells in the *Sox2-Cre;Fam20a*$^{fl/fl}$ mice. The *Fam20a*$^{fl/fl}$ mice from the same litters were used as controls. Both male and female mice were used in this study.

Mouse genotyping was performed by PCR analyses of genomic DNA extracted from tail biopsies, as previously described (Hayashi et al. 2002; Li et al. 2016). All animal procedures were approved by the Institutional Animal Care and Use Committee of Texas A&M University College of Dentistry (Dallas, TX, USA) and performed in accordance with the National Institutes of Health Guide for the Care and Use of Laboratory Animals.

Plain X-ray Radiography and Micro-computed Tomography (μCT)

The mandibles dissected from 7-week-old *Fam20a*$^{fl/fl}$ and *Sox2-Cre;Fam20a*$^{fl/fl}$ mice were analyzed with plain x-ray radiography (Faxitron Bioptics, Tucson, AZ, USA) and μCT (μCT35, Scanco Medical, Brüttisellen, Switzerland), as we previously described (Bouxsein et al. 2010; Gibson et al. 2013; Zhang et al. 2018).

Tissue Processing and Histological Analyses

The mouse mandibles were processed for standard paraffin embedding, and 5-μm serial sections were cut and used for Hematoxylin and Eosin (H&E) staining, *in situ* hybridization (ISH) and immunohistochemistry (IHC).

ISH was performed to examine the expressions of *Fam20a*, amelogenin (*Amel*), ameloblastin (*Ambn*), enamelin (*Enam*), amelotin (*Amtn*), dentin matrix protein 1 (*Dmp1*), and dentin sialophosphoprotein (*Dspp*), as previously described (Li et al. 2016; Liang et al. 2019; Wang et al. 2012b). Briefly, RNA probes were labeled with digoxigenin (DIG) using a RNA labeling kit (Roche Life Science, IN, USA), and the hybridized DIG-labeled RNA probes were detected by an enzyme-linked immunoassay with a specific anti-DIG-alkaline phosphatase antibody conjugate (Roche Life Science) and a blue alkaline phosphatase chromogen (BCIP/NBT) substrate (Vector Laboratories). The blue color indicated positive signals. Sections were counterstained with nuclear fast red. Three individual mice were analyzed for each genotype of mice.

IHC was carried out to detect AMEL, AMBN DMP1, DSP/DSPP and FAM20C using a mouse monoclonal anti-AMEL antibody (Santa Cruz Biotechnology; 1:500), a rabbit polyclonal anti-AMBN antibody (Santa Cruz Biotechnology; 1:500), rabbit anti-DMP1 polyclonal antibody (857–3) (Gibson et al. 2013), a rabbit anti-DSP polyclonal antibody (recognizing both DSP and full-length DSPP) (Gibson et al. 2013; Meng et al. 2015; Zhang et al. 2018), and a FAM20C rabbit polyclonal antibody (Wang et al. 2010), respectively. All the IHC experiments were performed using the DAB (3,3’-diaminobenzidine) kit (Vector Laboratories; Burlingame, CA), according to the manufacturer’s instructions. Three individual mice were analyzed for each genotype of mice.

Quantitative Real-time PCR (qPCR)

Total RNAs were extracted from the enamel organ tissues of the mandibular incisors of 3-day-old *Fam20a*$^{fl/fl}$ and *Sox2-Cre;Fam20a*$^{fl/fl}$ mice using an RNeasy mini kit (Qiagen, Hilden, Germany), and were reverse-transcribed into cDNAs using a QuantiTect reverse transcription kit (Qiagen). qPCR was performed on a Bio-Rad CFX96 system (Bio-Rad, California, USA) using SYBR green master mix (Promega, Wisconsin) to detect the mRNA levels of AMEL, AMBN, ENAM and AMTN. Ct values were normalized to the

housekeeping gene GAPDH, and expressed as fold changes compared to the experimental controls. The primers used for AMEL were (forward) 5'-CCCCAGTCACCTCTGCATC-3' and (reverse) 5'-GCTGCATGGAGAACAGTGG-3'; for AMBN (forward) 5'-TTGAGCCTTGAGACAATGAGAC −3' and (reverse) 5'-AAGTCCGTGCAACCATAAACTAT-3'; for ENAM (forward) 5'-TGCAGAAATCCGACTTCTCCT-3' and (reverse) 5'-CATCTGGAATGGCATGGCA-3'; for AMTN (forward) 5'-ATCAGCCCAGTCATTACCAAAG-3' and (reverse) 5'-AGGTCTGACCCCAGAGTGAG-3'; for GAPDH, (forward) 5'-CTCCTGGAAGATGGTGATGG-3', and (reverse) 5'-GGCAAAGTGGAGATTGTTGC-3'. Three independent mice were analyzed for each genotype of mice.

Western immunoblotting Analyses

Western immunoblotting was performed, as we previously described (Liang et al. 2016; Wang et al. 2010). For Western immunoblotting analyses of DMP1 and DSP/DSPP, total proteins were extracted from the maxillary and mandibular first molars of the 3-week-old *Fam20a*$^{fl/fl}$ and *Sox2-Cre;Fam20a*$^{fl/fl}$ mice, as described in our previous publications (Liang et al. 2019; Qin et al. 2001; Sun et al. 2010). For Western immunoblotting analysis of FAM20C, total proteins were extracted from the enamel organ tissues of the mandibular incisors of 3-day-old *Fam20a*$^{fl/fl}$ and *Sox2-Cre;Fam20a*$^{fl/fl}$ mice. Western immunoblotting was then performed to detect DMP1 and DSP/DSPP using rabbit polyclonal antibodies described above, and FAM20C using a FAM20C rabbit polyclonal antibody, as previously described (Wang et al. 2010). The secondary antibodies were horseradish peroxidase (HRP)-conjugated goat anti-rabbit IgG (Santa Cruz Biotechnology; 1:1000). β-actin was immunoblotted with mouse monoclonal anti-β-actin-peroxidase antibody (Sigma; 1:20,000). The immunoreactive protein bands were visualized with ECL™ Chemiluminescent Detection reagents (Amersham Biosciences, Illinois, USA) and imaged using a CL-XPosure film (Pierce Biotechnology, Inc., New Jersey, USA). Three independent mice were analyzed for each genotype and antibody, and one representative experiment was shown.

Statistical Analysis

Student's t-test was used to compare the means between two groups. Data were expressed as mean ± standard deviation (SD). $P < 0.05$ was considered statistically significant.

Results

Generation of the *Sox2-Cre;Fam20a*$^{fl/fl}$ Mice

To study the functions of FAM20A in ameloblasts and odontoblasts during tooth development, we generated a *Fam20a* knockout mice (*Sox2-Cre;Fam20a*$^{fl/fl}$) by breeding *Fam20a*$^{fl/fl}$ mice with *Sox2-Cre* transgenic mice. *In situ* hybridization showed strong signals of FAM20A mRNA in the ameloblasts and odontoblasts in the 4-day-old *Fam20a*$^{fl/fl}$ control mice (Fig. 1A and A1), whereas FAM20A mRNA signals were not detected in the age-matched *Sox2-Cre;Fam20a*$^{fl/fl}$ mice (Fig. 1B and B1). These data demonstrated that *Fam20a* was effectively ablated in both ameloblasts and odontoblasts of the *Sox2-Cre;Fam20a*$^{fl/fl}$ mice.

The *Sox2-Cre;Fam20a$^{fl/fl}$* mice displayed severe enamel defects

Having established the *Fam20a* knockout mice, we examined the overall enamel phenotype of 7-week-old *Sox2-Cre;Fam20a$^{fl/fl}$* mice. Compared with the *Fam20a$^{fl/fl}$* mice, the incisors of *Sox2-Cre;Fam20a$^{fl/fl}$* mice displayed a chalky white and opaque appearance (Fig. 2A and B), and their molars showed a yellowish and rough surface, likely resulting from the loss of enamel and exposure of the underlying dentin (Fig. 2C and D). Plain x-ray radiography demonstrated that the mandibular molars had sharp cusps in the *Fam20a$^{fl/fl}$* mice, but the molar cusps became blunt in the *Sox2-Cre;Fam20a$^{fl/fl}$* mice (Fig. 2E and F). Moreover, a distinct band of ectopic calcifications was found between the labial aspect of the mandibular incisor and alveolar bone in the *Sox2-Cre;Fam20a$^{fl/fl}$* mice, but not in the *Fam20a$^{fl/fl}$* mice.

Furthermore, μCT analyses were performed on the mandibular incisors at three different transverse locations that represent the enamel formation at the late secretory stage, late maturation stage and early tooth eruption stage (enamel mineral density reaches its peak), respectively (Fig. 2E and F). The trans-axial μCT images showed that, at the late secretory stage, no enamel was found in either the *Fam20a$^{fl/fl}$* or *Sox2-Cre;Fam20a$^{fl/fl}$* mice (Fig. 2E1 and F1). At the late maturation stage, the incisors showed a distinct layer of enamel formed on their labial side in the *Fam20a$^{fl/fl}$* mice whereas a layer of ectopic calcifications, in place of normal enamel, was found in the *Sox2-Cre;Fam20a$^{fl/fl}$* mice (Fig. 2E2 and F2). At the early tooth eruption stage, the incisors had well-formed enamel in the *Fam20a$^{fl/fl}$* mice, whereas the ectopic calcifications remained on the labial side of the incisors in the *Sox2-Cre;Fam20a$^{fl/fl}$* mice (Fig. 2E3 and F3). In addition, the mandibular first molars showed the presence of nicely-formed enamel in the *Fam20a$^{fl/fl}$* mice (Fig. 2E2), but the absence of enamel in the *Sox2-Cre;Fam20a$^{fl/fl}$* mice (Fig. 2F2). Altogether, these results demonstrated that deletion of *Fam20a* in both dental epithelium and dental mesenchyme resulted in a severe human AI-like enamel phenotype.

Ameloblast morphological changes in the *Sox2-Cre;Fam20a$^{fl/fl}$* mice

To understand the pathogenic mechanism associated with the enamel defects, we examined the morphological changes of the ameloblasts in the 7-day-old *Sox2-Cre;Fam20a$^{fl/fl}$* mouse mandibular incisors as the incisors continue to erupt in mice. H&E staining showed that the secretory stage ameloblasts of the *Fam20a$^{fl/fl}$* mice exhibited a high columnar shape with Tomes' process on their apical ends (Fig. 3A and A1). However, the secretory stage amelobasts of the *Sox2-Cre;Fam20a$^{fl/fl}$* mice became remarkably shorter, lacked Tomes' process, and detached from the enamel matrix (Fig. 3B and B1). The maturation stage ameloblasts of the *Fam20a$^{fl/fl}$* mice were shorter, but remained polarized with their apical ends against the enamel matrix (Fig. 3A and A2), whereas the maturation stage ameloblasts in the *Sox2-Cre;Fam20a$^{fl/fl}$* mice completely lost their polarity, became highly disorganized, and formed numerous spherical foci of extracellular matrix (Fig. 3B and B2). Consistent with the pathological changes in ameloblast morphology, the ameloblasts only deposited a very thin layer of enamel matrix in the *Sox2-Cre;Fam20a$^{fl/fl}$* mice, compared to those in the *Fam20a$^{fl/fl}$* mice (Fig. 3). Therefore, loss of FAM20A function resulted in dramatic changes in ameloblast morphology in the *Sox2-Cre;Fam20a$^{fl/fl}$* mice.

Reduced expression levels of the secretory and maturation stage ameloblast markers in the *Sox2-Cre;Fam20a$^{fl/fl}$* mice

At the molecular level, we analyzed the expressions of the secretory and maturation stage ameloblast markers, including AMEL, AMBN, ENAM and AMTN, by ISH, qPCR and/or IHC. Both ISH and qPCR showed that the mRNA levels of AMEL, AMBN, ENAM and AMTN were remarkably decreased in the *Sox2-Cre;Fam20a$^{fl/fl}$* mice, compared to the *Fam20a$^{fl/fl}$* mice (Figs. 4 and 5). Immunohistochemistry further demonstrated that there was a dramatic reduction in both AMEL and AMBN protein levels in the enamel matrix and/or within ameloblasts (Fig. 6). Interestingly, at the maturation stage of amelogenesis, even though the ameloblasts lost their polarity, they continue to express the secretory and maturation stage ameloblast markers, including AMEL, AMBN, ENAM and AMTN, and formed spherical foci of ectopic enamel matrix in the *Sox2-Cre;Fam20a$^{fl/fl}$* mice (Figs. 4 and 6). These abnormal maturation stage ameloblasts in the *Sox2-Cre;Fam20a$^{fl/fl}$* mice did not express type I collagen or DMP1 – two markers for osteocytes/odontoblasts (Online Resource Fig. 1A–D; and A1–D1), and they did not show increased cell proliferation or apoptosis (Online Resource Fig. 2A–E; and A1–E1). Collectively, these findings indicate that although the secretory stage ameloblasts became shorter, and expressed reduced levels of the secretory stage ameloblast markers, they were still capable of differentiating into the ameloblasts that expressed the marker for the maturation stage ameloblasts in the *Sox2-Cre;Fam20a$^{fl/fl}$* mice.

The *Sox2-Cre;Fam20a$^{fl/fl}$* mice had no obvious defects in dentin and odontoblast differentiation

Next, we examined the dentin phenotype of the *Sox2-Cre;Fam20a$^{fl/fl}$* mice as *Fam20a* is deleted in the odontoblasts in these mice. Interestingly, the trans-axial μCT images showed no apparent difference in dentin formation at different locations in the mandibular incisor of the *Sox2-Cre;Fam20a$^{fl/fl}$* mice (Fig. 2F1–F3), compared to the corresponding locations in the *Fam20a$^{fl/fl}$* mice (Fig. 2E1–E3). Furthermore, quantitative μCT analyses revealed that there were no significant differences in the dentin/cementum volume (Online Resource Fig. 3A) and density (Online Resource Fig. 3B) of the mandibular incisors between the *Fam20a$^{fl/fl}$* and *Sox2-Cre;Fam20a$^{fl/fl}$* mice. To further determine whether there were any pathological changes in dentin formation, we performed histological and molecular analyses of the odontobolasts in 3-week-old *Fam20a$^{fl/fl}$* and *Sox2-Cre;Fam20a$^{fl/fl}$* mice. H&E staining showed that the odontoblasts in the *Sox2-Cre;Fam20a$^{fl/fl}$* mice exhibited a similar morphology as those in the *Fam20a$^{fl/fl}$* mice (Fig. 7A, A1, B and B1). IHC, ISH and Western immunoblotting assays demonstrated that the odontoblasts expressed comparable levels of the odontoblast differentiation markers, DMP1 and DSPP, in the *Fam20a$^{fl/fl}$* and *Sox2-Cre;Fam20a$^{fl/fl}$* mice (Fig. 7C–J and C1-F1; and Fig. 8). Taken together, these observations indicate that *Fam20a* ablation in the odontoblasts had no apparent effects on dentin formation and odontoblast differentiation.

Reduced levels of FAM20C in the *Sox2-Cre;Fam20a$^{fl/fl}$* mice

Previous *in vitro* studies suggest that FAM20A binds to FAM20C and regulates FAM20C localization (Ohyama et al. 2016). Therefore, we analyzed FAM20C protein in the

mandibular incisors in the *Sox2-Cre;Fam20a*$^{fl/fl}$ mice by IHC and Western immunoblotting assays. IHC showed that FAM20C protein level was dramatically reduced in the secretory and maturation stage ameloblasts as well as odontoblasts in the *Sox2-Cre;Fam20a*$^{fl/fl}$ mice, compared to the *Fam20a*$^{fl/fl}$ mice (Fig. 9A, B, A1, A2, B1 and B2). However, there was no apparent difference in FAM20C protein distribution in the ameloblasts and odontoblasts in the *Sox2-Cre;Fam20a*$^{fl/fl}$ mice, compared to the *Fam20a*$^{fl/fl}$ mice (Fig. 9A, B, A1, A2, B1 and B2). Western immunoblotting assay further confirmed the marked reduction in FAM20C protein level in the enamel organs of the mandibular incisors of the 3-day-old *Sox2-Cre;Fam20a*$^{fl/fl}$ mice, compared to the age-matched *Fam20a*$^{fl/fl}$ mice (Fig. 9C). These results indicate that *Fam20a* deletion caused a marked decrease in *Fam20c* expression, but it did not alter FAM20C protein localization in the ameloblasts and odontoblasts.

DISCUSSION

In this study, we created a *Fam20a* knockout mouse model (*Sox2-Cre;Fam20a*$^{fl/fl}$), in which *Fam20a* was ablated in both ameloblasts and odontoblasts. We demonstrated that the *Sox2-Cre;Fam20a*$^{fl/fl}$ mice developed a human AI-like enamel phenotype, but did not exhibit apparent dentin defects.

To study the cellular and molecular mechanisms underlying the enamel defects associated with *Fam20a* ablation, we took advantage of the continuously growing mouse mandibular incisors. At the cellular level, we found that the secretory stage ameloblasts in the *Sox2-Cre;Fam20a*$^{fl/fl}$ mice were shorter and detached from the enamel matrix, but they continued to differentiate into the ameloblasts that expressed the marker for the maturation stage ameloblasts and were disorganized and formed numerous spherical foci of enamel matrices. At the molecular level, we showed that the *Sox2-Cre;Fam20a*$^{fl/fl}$ mice had remarkably reduced expressions of the genes encoding the secretory and maturation stage ameloblast markers, including *Amel*, *Ambn*, *Enam* and *Amtn*. As a consequence of the pathological changes in ameloblasts, only a very thin layer of enamel matrix was deposited in the *Sox2-Cre;Fam20a*$^{fl/fl}$ mice. Interestingly, even though the maturation stage ameloblasts in the *Sox2-Cre;Fam20a*$^{fl/fl}$ mice were abnormal and highly disorganized, they showed no increase in either cell proliferation or apoptosis. The enamel defects of the *Sox2-Cre;Fam20a*$^{fl/fl}$ mice resemble those in the *Sox2-Cre;Fam20c*$^{fl/fl}$ mice (Wang et al. 2012b), which seems to support a functional relationship between FAM20A and FAM20C.

To date, two molecular mechanisms have been proposed to explain the functional interaction between FAM20A and FAM20C. First, it is thought that FAM20A binds to FAM20C and regulates FAM20C localization (Ohyama et al. 2016). However, by immunohistochemistry, we demonstrated that although the FAM20C protein levels were dramatically reduced in both ameloblasts and odontoblasts, FAM20C displayed a similar intracellular localization in the *Sox2-Cre;Fam20a*$^{flox/flox}$ mice and control mice. This finding is consistent with the previous report showing that FAM20C is localized and functions intracellularly within ameloblasts and odontoblasts (Wang et al. 2013b). Secondly, FAM20A forms a complex with FAM20C and increases the kinase activity of the latter in phosphorylating secretory calcium-binding phosphoproteins (SCPPs), including enamel matrix proteins (Cui et al. 2015). Although *in vitro* studies support that FAM20A and FAM20C form a functional

complex, whether such a complex forms and functions similarly *in vivo*, particularly in ameloblasts and odontoblasts, is not known.

The data obtained from the current study and others challenge the role of FAM20A in enhancing the kinase activity of FAM20C in phosphorylating SCPPs *in vivo*. First, the enamel matrix proteins, including AMBN and ENAM, have a few "Ser-x-Glu/pSer" motifs that may be potentially phosphorylated by FAM20C in ameloblasts, which is presumably assisted by FAM20A. Nevertheless, the fate of the ameloblasts in the *Sox2-Cre;Fam20a*$^{flox/flox}$ mice was quite different from that observed in either *Ambn*-null (Fukumoto et al. 2004) or *Enam*-null (Hu et al. 2011). The ameloblasts resumed cell proliferation following detachment from the enamel matrix in the *Ambn*-null mice (Fukumoto et al. 2004), whereas the ameloblasts underwent apoptosis in the *Enam*-null mice (Hu et al. 2011). These observations suggest that the enamel phenotype of the *Sox2-Cre;Fam20a*$^{flox/flox}$ mice cannot be simply explained by the loss of enamel matrix protein phosphorylation. Secondly, DMP1 and DSPP are abundantly produced by the odontoblasts. Compared to the enamel matrix proteins, DMP1 and DSPP are highly phosphorylated (Butler et al. 1983; Qin et al. 2003). Thus, the odontoblasts need FAM20A much greater than the ameloblasts if the kinase activity of FAM20C requires the assistance of FAM20A. However, even though *Fam20a* is co-expressed with *Fam20c* in odontoblasts (Li et al. 2016; Wang et al. 2010), we showed that *Fam20a* inactivation did not affect the expression levels of DMP1 and DSPP at the mRNA and protein levels or cause apparent dentin defects. This finding is consistent with the previous reports on the dentin phenotypes of conventional *Fam20a* knockout mice (Vogel et al. 2012) and *Fam20a*-deficient human subjects (Wang et al. 2013a). However, these observations are paradoxical with the finding that *Fam20c* ablation causes severe dentin defects in mice (Wang et al. 2012b), given that FAM20A forms a complex with FAM20C and enhances FAM20C kinase activity. Lastly, there are other phenotypic differences between the *Fam20a*- and *Fam20c*-deficient subjects. Skeletal abnormalities and cerebral calcification are often observed in *Fam20c*-deficient human patients and mice (Ababneh et al. 2013; Faundes et al. 2014; Wang et al. 2012a), but have not been reported in *Fam20a*-deficient subjects so far. Altogether, although our current studies do not exclude the possibility that FAM20A may form a complex with FAM20C and enhances the kinase activity of FAM20C in phosphorylating enamel matrix proteins in ameloblasts, the mechanistic link between FAM20A and FAM20C *in vivo* indeed needs to be further investigated in the future.

In summary, we showed that FAM20A is essential for amelogenesis, but is dispensable for dentinogenesis. Future studies are warranted to further determine the functional difference of FAM20A in amelogenesis and dentinogenesis as well as the functional interaction of FAM20A and FAM20C in amelogenesis.

Supplementary Material

Refer to Web version on PubMed Central for supplementary material.

ACKNOWLEDGEMENTS

This work was supported by National Institute of Dental and Craniofacial Research [grant numbers DE022549 (to CQ), DE027345 (to YL and CQ)]. L.L. and S.F. contributed to design, data acquisition, analysis and interpretation, drafted and critically revised the manuscript. H.Z. and S.W. contributed to data acquisition, analysis, drafted and critically revised the manuscript; Q.X. contributed to data acquisition, analysis and critically revised the manuscript; C.Q. contributed to conception, interpretation, drafted and critically revised the manuscript; Y.L. contributed to conception, design, interpretation, drafted and critically revised the manuscript. All authors approved the final version of the submitted manuscript and agreed to be accountable for all aspects of the work. The authors declare that they have no conflict of interest with respect to the content of this article.

REFERENCES

Ababneh FK, AlSwaid A, Youssef T, Al Azzawi M, Crosby A, AlBalwi MA. 2013 Hereditary deletion of the entire fam20c gene in a patient with raine syndrome. Am J Med Genet A. 161A(12):3155–3160. [PubMed: 24039075]

Bouxsein ML, Boyd SK, Christiansen BA, Guldberg RE, Jepsen KJ, Muller R. 2010 Guidelines for assessment of bone microstructure in rodents using micro-computed tomography. J Bone Miner Res. 25(7):1468–1486. [PubMed: 20533309]

Butler WT, Bhown M, DiMuzio MT, Cothran WC, Linde A. 1983 Multiple forms of rat dentin phosphoproteins. Archives of biochemistry and biophysics. 225(1):178–186. [PubMed: 6614917]

Cui J, Xiao J, Tagliabracci VS, Wen J, Rahdar M, Dixon JE. 2015 A secretory kinase complex regulates extracellular protein phosphorylation. Elife. 4:e06120. [PubMed: 25789606]

Faundes V, Castillo-Taucher S, Gonzalez-Hormazabal P, Chandler K, Crosby A, Chioza B. 2014 Raine syndrome: An overview. Eur J Med Genet. 57(9):536–542. [PubMed: 25019372]

Fukumoto S, Kiba T, Hall B, Iehara N, Nakamura T, Longenecker G, Krebsbach PH, Nanci A, Kulkarni AB, Yamada Y. 2004 Ameloblastin is a cell adhesion molecule required for maintaining the differentiation state of ameloblasts. J Cell Biol. 167(5):973–983. [PubMed: 15583034]

Gibson MP, Zhu Q, Wang S, Liu Q, Liu Y, Wang X, Yuan B, Ruest LB, Feng JQ, D'Souza RN et al. 2013 The rescue of dentin matrix protein 1 (dmp1)-deficient tooth defects by the transgenic expression of dentin sialophosphoprotein (dspp) indicates that dspp is a downstream effector molecule of dmp1 in dentinogenesis. The Journal of biological chemistry. 288(10):7204–7214. [PubMed: 23349460]

Hayashi S, Lewis P, Pevny L, McMahon AP. 2002 Efficient gene modulation in mouse epiblast using a sox2cre transgenic mouse strain. Mech Dev. 119 Suppl 1:S97–S101. [PubMed: 14516668]

Hu JC, Lertlam R, Richardson AS, Smith CE, McKee MD, Simmer JP. 2011 Cell proliferation and apoptosis in enamelin null mice. Eur J Oral Sci. 119 Suppl 1:329–337. [PubMed: 22243264]

Ishikawa HO, Xu A, Ogura E, Manning G, Irvine KD. 2012 The raine syndrome protein fam20c is a golgi kinase that phosphorylates bio-mineralization proteins. PLoS One. 7(8):e42988. [PubMed: 22900076]

Jaureguiberry G, De la Dure-Molla M, Parry D, Quentric M, Himmerkus N, Koike T, Poulter J, Klootwijk E, Robinette SL, Howie AJ et al. 2012 Nephrocalcinosis (enamel renal syndrome) caused by autosomal recessive fam20a mutations. Nephron Physiol. 122(1–2):1–6. [PubMed: 23434854]

Kantaputra PN, Kaewgahya M, Khemaleelakul U, Dejkhamron P, Sutthimethakorn S, Thongboonkerd V, Iamaroon A. 2014 Enamel-renal-gingival syndrome and fam20a mutations. Am J Med Genet A. 164A(1):1–9. [PubMed: 24259279]

Koike T, Izumikawa T, Tamura J, Kitagawa H. 2009 Fam20b is a kinase that phosphorylates xylose in the glycosaminoglycan-protein linkage region. Biochem J. 421(2):157–162. [PubMed: 19473117]

Li LL, Liu PH, Xie XH, Ma S, Liu C, Chen L, Qin CL. 2016 Loss of epithelial fam20a in mice causes amelogenesis imperfecta, tooth eruption delay and gingival overgrowth. Int J Oral Sci. 8(2):98–109. [PubMed: 27281036]

Liang T, Meng T, Wang S, Qin C, Lu Y. 2016 The lpv motif is essential for the efficient export of secretory dmp1 from the endoplasmic reticulum. Journal of cellular physiology. 231(7):1468–1475. [PubMed: 26595451]

Liang T, Zhang H, Xu Q, Wang S, Qin C, Lu Y. 2019 Mutant dentin sialophosphoprotein causes dentinogenesis imperfecta. J Dent Res.22034519854029.

Meng T, Huang Y, Wang S, Zhang H, Dechow PC, Wang X, Qin C, Shi B, D'Souza RN, Lu Y. 2015 Twist1 is essential for tooth morphogenesis and odontoblast differentiation. The Journal of biological chemistry. 290(49):29593–29602. [PubMed: 26487719]

O'Sullivan J, Bitu CC, Daly SB, Urquhart JE, Barron MJ, Bhaskar SS, Martelli-Junior H, dos Santos Neto PE, Mansilla MA, Murray JC et al. 2011 Whole-exome sequencing identifies fam20a mutations as a cause of amelogenesis imperfecta and gingival hyperplasia syndrome. Am J Hum Genet. 88(5):616–620. [PubMed: 21549343]

Ohyama Y, Lin JH, Govitvattana N, Lin IP, Venkitapathi S, Alamoudi A, Husein D, An C, Hotta H, Kaku M et al. 2016 Fam20a binds to and regulates fam20c localization. Sci Rep. 6:27784. [PubMed: 27292199]

Qin C, Brunn JC, Cook RG, Orkiszewski RS, Malone JP, Veis A, Butler WT. 2003 Evidence for the proteolytic processing of dentin matrix protein 1. Identification and characterization of processed fragments and cleavage sites. J Biol Chem. 278(36):34700–34708. [PubMed: 12813042]

Qin C, Cook RG, Orkiszewski RS, Butler WT. 2001 Identification and characterization of the carboxyl-terminal region of rat dentin sialoprotein. J Biol Chem. 276(2):904–909. [PubMed: 11042175]

Simpson MA, Hsu R, Keir LS, Hao J, Sivapalan G, Ernst LM, Zackai EH, Al-Gazali LI, Hulskamp G, Kingston HM et al. 2007 Mutations in fam20c are associated with lethal osteosclerotic bone dysplasia (raine syndrome), highlighting a crucial molecule in bone development. Am J Hum Genet. 81(5):906–912. [PubMed: 17924334]

Simpson MA, Scheuerle A, Hurst J, Patton MA, Stewart H, Crosby AH. 2009 Mutations in fam20c also identified in non-lethal osteosclerotic bone dysplasia. Clin Genet. 75(3):271–276. [PubMed: 19250384]

Sun Y, Lu Y, Chen S, Prasad M, Wang X, Zhu Q, Zhang J, Ball H, Feng J, Butler WT et al. 2010 Key proteolytic cleavage site and full-length form of dspp. Journal of dental research. 89(5):498–503. [PubMed: 20332332]

Tagliabracci VS, Engel JL, Wen J, Wiley SE, Worby CA, Kinch LN, Xiao J, Grishin NV, Dixon JE. 2012 Secreted kinase phosphorylates extracellular proteins that regulate biomineralization. Science. 336(6085):1150–1153. [PubMed: 22582013]

Tagliabracci VS, Wiley SE, Guo X, Kinch LN, Durrant E, Wen J, Xiao J, Cui J, Nguyen KB, Engel JL et al. 2015 A single kinase generates the majority of the secreted phosphoproteome. Cell. 161(7): 1619–1632. [PubMed: 26091039]

Vogel P, Hansen GM, Read RW, Vance RB, Thiel M, Liu J, Wronski TJ, Smith DD, Jeter-Jones S, Brommage R. 2012 Amelogenesis imperfecta and other biomineralization defects in fam20a and fam20c null mice. Vet Pathol. 49(6):998–1017. [PubMed: 22732358]

Wang SK, Aref P, Hu Y, Milkovich RN, Simmer JP, El-Khateeb M, Daggag H, Baqain ZH, Hu JC. 2013a Fam20a mutations can cause enamel-renal syndrome (ers). PLoS Genet. 9(2):e1003302. [PubMed: 23468644]

ang SK, Reid BM, Dugan SL, Roggenbuck JA, Read L, Aref P, Taheri AP, Yeganeh MZ, Simmer JP, Hu JC. 2014 Fam20a mutations associated with enamel renal syndrome. J Dent Res. 93(1):42–48. [PubMed: 24196488]

Wang SK, Samann AC, Hu JC, Simmer JP. 2013b Fam20c functions intracellularly within both ameloblasts and odontoblasts in vivo. J Bone Miner Res. 28(12):2508–2511. [PubMed: 23703840]

Wang X, Hao J, Xie Y, Sun Y, Hernandez B, Yamoah AK, Prasad M, Zhu Q, Feng JQ, Qin C. 2010 Expression of fam20c in the osteogenesis and odontogenesis of mouse. J Histochem Cytochem. 58(11):957–967. [PubMed: 20644212]

Wang X, Jung J, Liu Y, Yuan B, Lu Y, Feng JQ, Qin C. 2013c The specific role of fam20c in amelogenesis. J Dent Res. 92(11):995–999. [PubMed: 24026952]

Wang X, Wang S, Li C, Gao T, Liu Y, Rangiani A, Sun Y, Hao J, George A, Lu Y et al. 2012a Inactivation of a novel fgf23 regulator, fam20c, leads to hypophosphatemic rickets in mice. PLoS Genet. 8(5):e1002708. [PubMed: 22615579]

Wang X, Wang S, Lu Y, Gibson MP, Liu Y, Yuan B, Feng JQ, Qin C. 2012b Fam20c plays an essential role in the formation of murine teeth. J Biol Chem. 287(43):35934–35942. [PubMed: 22936805]

Zhang H, Xie X, Liu P, Liang T, Lu Y, Qin C. 2018 Transgenic expression of dentin phosphoprotein (dpp) partially rescued the dentin defects of dspp-null mice. PLoS One. 13(4):e0195854. [PubMed: 29672573]

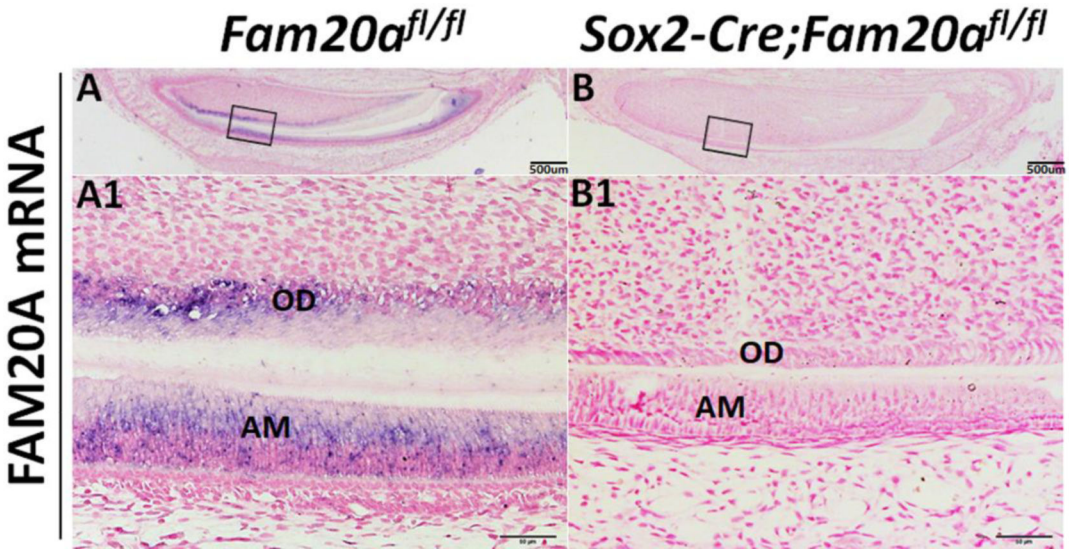

Fig. 1. *In situ* hybridization analysis of FAM20A mRNA in the mandibular incisors of the *Fam20a*$^{fl/fl}$ and *Sox2-Cre;Fam20a*$^{fl/fl}$ mice

Shown are the *in situ* hybridization results (signal in purple) of FAM20A mRNA on the sagittal sections of the mandibular incisors of 4-day-old *Fam20a*$^{fl/fl}$ (A) and *Sox2-Cre;Fam20a*$^{fl/fl}$ (B) mice. A1 and B1 are the higher magnification views of the boxed areas in A and B, respectively. FAM20A mRNA signals were strongly detected in the ameloblasts and odontoblasts in the *Fam20a*$^{fl/fl}$ mice, but they were undetectable in the *Sox2-Cre;Fam20a*$^{fl/fl}$ mice. Abbreviations: AM, ameloblasts; and OD, odontoblasts. Scale bars: 500 μm in A and B; 50 μm in A1 and B1.

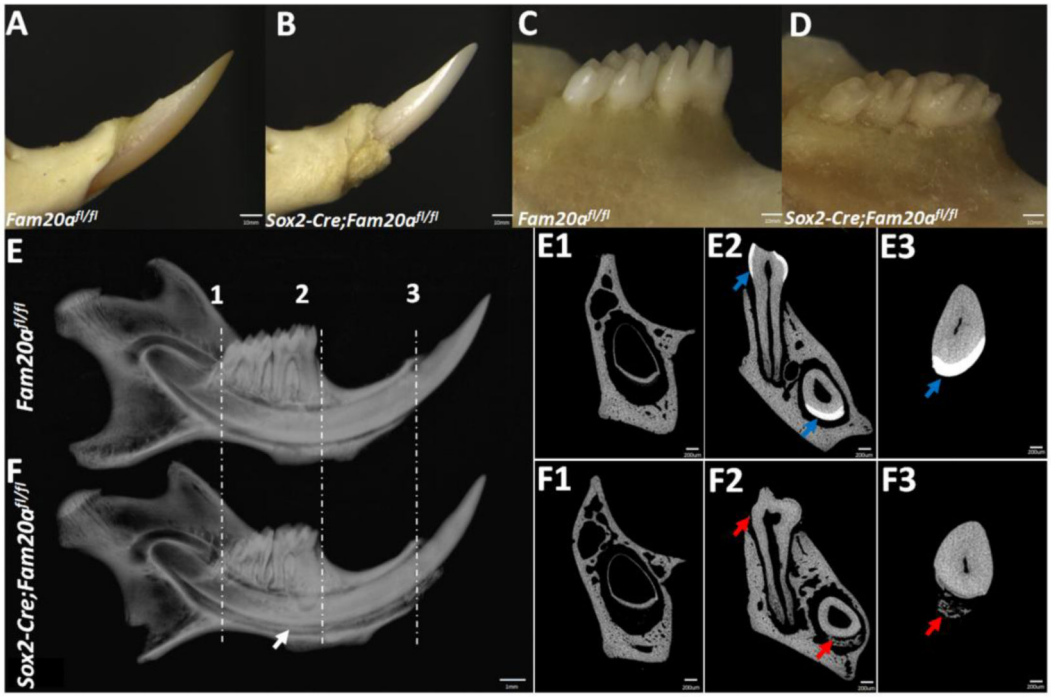

Fig. 2. Gross analyses of the tooth phenotype of the *Sox2-Cre;Fam20a*$^{fl/fl}$ mice

A-D, representative photographs of the mandibular incisors (A and B) and mandibular molars (C and D) of 7-week-old *Fam20a*$^{fl/fl}$ (A and C) and *Sox2-Cre;Fam20a*$^{fl/fl}$ (B and D) mice. E and F, representative plain x-ray radiographic images of the mandibles of 7-week-old *Fam20a*$^{fl/fl}$ (E) and *Sox2-Cre;Fam20a*$^{fl/fl}$ (F) mice. The dashed lines mark the different stages of enamel formation for the mandibular incisors: the late secretory stage (line 1), late maturation stage (line 2), and early tooth eruption (line 3) stage, in which enamel mineral density reached the maximal point. E1-E3 and F1-F3 are the trans-axial μCT images at the locations that correspond to the three stages of incisor enamel formation in E and F, respectively. Note a distinct band of ectopic calcifications (pointed by the white arrow) observed between the labial aspect of the mandibular incisor and alveolar bone in the *Sox2-Cre;Fam20a*$^{fl/fl}$ mice (F) but not in the *Fam20a*$^{fl/fl}$ mice (E); also note the well-formed enamel (marked by blue arrows) in the mandibular first molars and incisors in the *Fam20a*$^{fl/fl}$ mice (E2 and E3), and the lack of enamel in the first molars or substitution of enamel with ectopic calcifications (pointed by red arrows) in the mandibular incisors in the *Sox2-Cre;Fam20a*$^{fl/fl}$ mice (F2 and F3). Scale bars: 10 mm in A-D; 1 mm in E and F; 200 μm in E1-E3 and F1-F3.

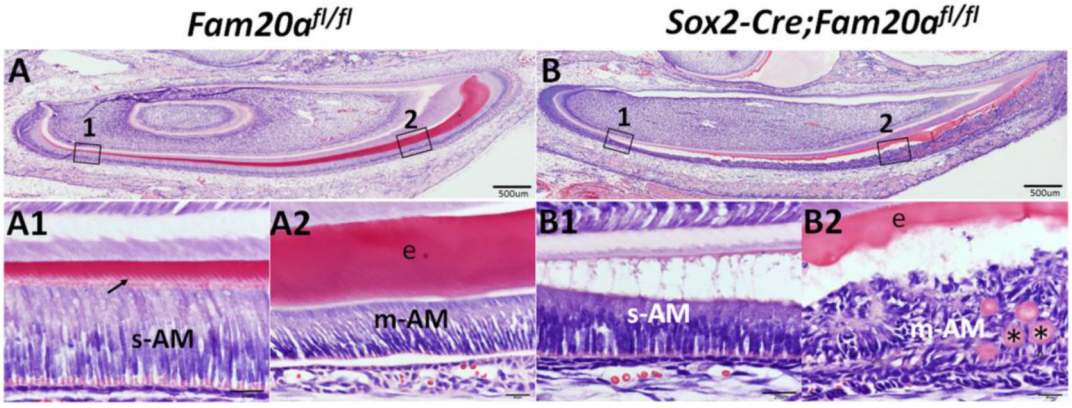

Fig. 3. H&E staining of the mandibular incisors

A and B, representative H&E staining of the sagittal sections of the mandibular incisors of 7-day-old *Fam20a*$^{fl/fl}$ (A) and *Sox2-Cre;Fam20a*$^{fl/fl}$ (B) mice. A1 and B1 are the higher magnification views of the secretory stage ameloblasts in boxes 1 in A and B, respectively. A2 and B2 are the higher magnification views of the maturation stage ameloblasts in boxes 2 in A and B, respectively. In the *Fam20a*$^{fl/fl}$ mice, Tomes' processes (pointed by black arrow in A1) were clearly visible, whereas they were lost in the *Sox2-Cre;Fam20a*$^{fl/fl}$ mice (B1). Spherical foci of ectopic extracellular matrix (marked by asterisks in B2) were formed in the *Sox2-Cre;Fam20a*$^{fl/fl}$ mice. Abbreviations: e, enamel; s-AM, secretory stage ameloblasts; and m-AM, maturation stage ameloblasts. Asterisks (*) mark the spherical ectopic calcifications. Scale bars: 500 μm in A and B; 20 μm in A1, A2, B1, and B2.

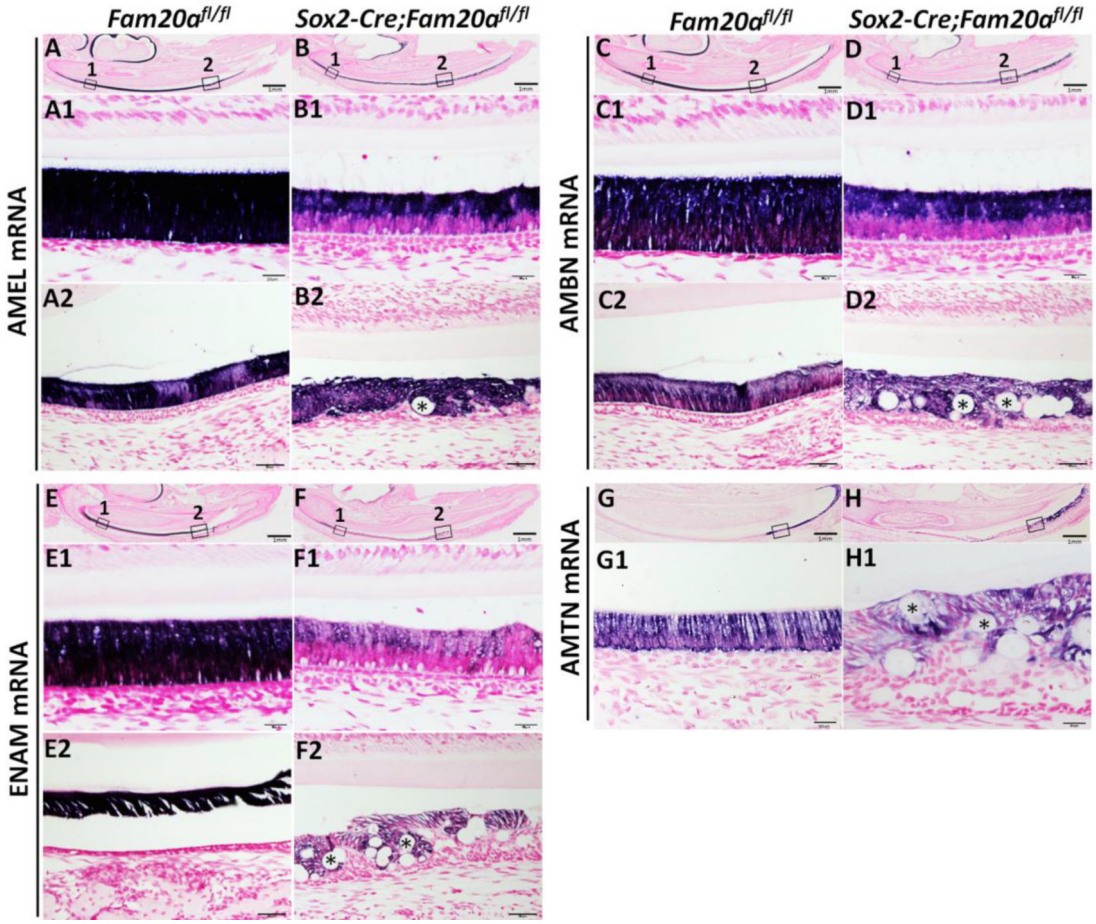

Fig. 4. *In situ* hybridization analyses of the secretory and maturation stage ameloblast markers

A-B, representative *in situ* hybridization results (signal in purple) of AMEL (A and B), AMBN (C and D), ENAM (E and F) and AMTN (G and H) on the sagittal sections of the mandibular incisors of 7-day-old *Fam20a*$^{fl/fl}$ (A, C, E and G) and *Sox2-Cre;Fam20a*$^{fl/fl}$ (B, D, F and H) mice. A1-F1 are the higher magnification views of the secretory stage ameloblasts in black boxes 1 in A-F, respectively. A2-F2 are the higher magnification views of the maturation stage ameloblasts in black boxes 2 in A-F, respectively. G1 and H1 are the higher magnification views of the maturation stage ameloblasts in black boxes in G and H, respectively. The levels of AMEL, AMBN and ENAM and AMTN mRNAs were dramatically decreased in the secretory and/or maturation stage ameloblasts in the *Sox2-Cre;Fam20a*$^{fl/fl}$ mouse incisors, compared to the *Fam20a*$^{fl/fl}$ mouse incisors. Asterisks (*) mark the spherical ectopic calcifications. Scale bars: 1 mm in A-H; 20 μm in A1-H1 and A2-F2.

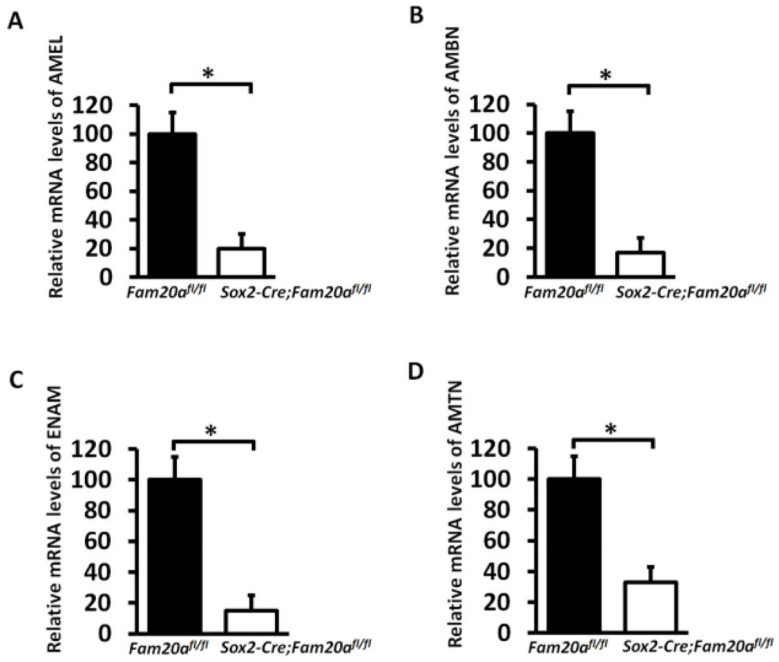

Fig. 5. qPCR analyses of the mRNA levels of the secretory and maturation stage ameloblast markers

qPCR analyses of AMEL (A), AMBN (B), ENAM (C) and AMTN (D) mRNA levels in the mandibular incisors of 7-day-old *Fam20a*$^{fl/fl}$ and *Sox2-Cre;Fam20a*$^{fl/fl}$ mice. n=4; The mRNA levels of the *Fam20a*$^{fl/fl}$ mice are set as 1; Values are mean ± SD. *: statistically different from the *Fam20a*$^{fl/fl}$ mice (α=0.05).

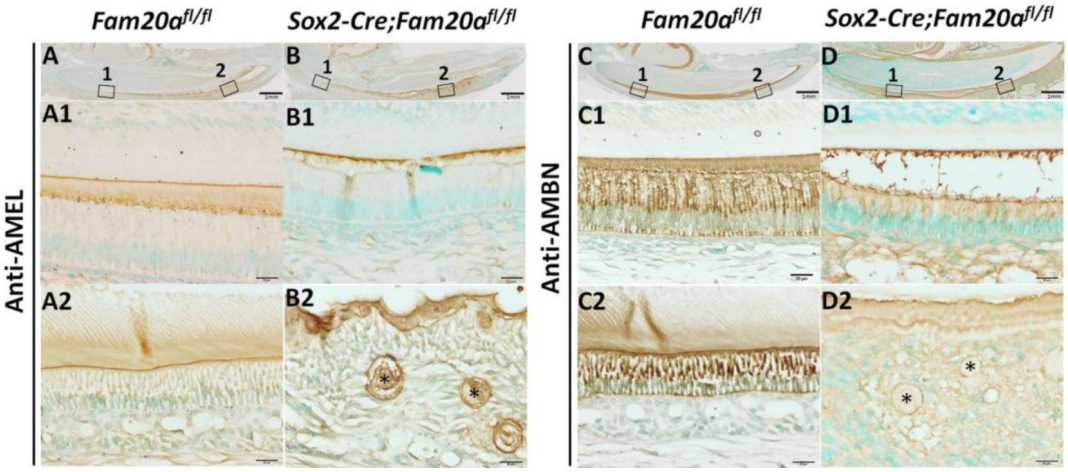

Fig. 6. Immunohistochemical analyses of AMEL and AMBN in the mandibular incisors

A-D, representative immunohistochemical results (signal in brown) of AMEL (A and B) and AMBN (C and D) on the sagittal sections of the mandibular incisors of 7-day-old *Fam20a*$^{fl/fl}$ (A and C) and *Sox2-Cre;Fam20a*$^{fl/fl}$ (B and D) mice. A1-D1 are the higher magnification views of the secretory stage ameloblasts in black boxes 1 in A-D, respectively. A2-D2 are the higher magnification views of the maturation stage ameloblasts in black boxes 2 in A-D, respectively. AMEL and AMBN proteins were markedly reduced in both secretory and maturation stage ameloblasts in the *Sox2-Cre;Fam20a*$^{fl/fl}$ mouse incisors, compared to the *Fam20a*$^{fl/fl}$ mouse incisors. Asterisks (*) mark the spherical ectopic calcifications. Scale bars: 1 mm in A-D; 20 μm in A1-D1 and A2-D2.

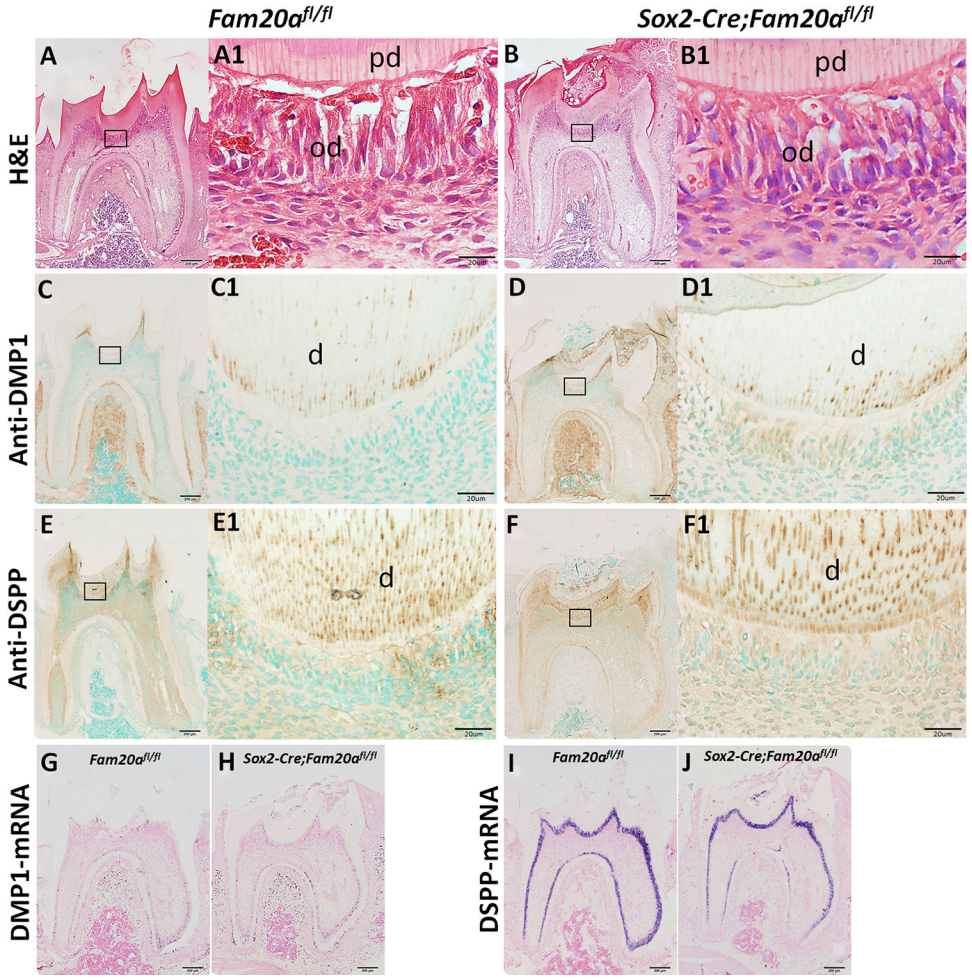

Fig. 7. Histological and molecular analyses of the odontoblalsts of the mandibular first molars

A and B, representative H&E staining images of the mandibular first molars of 3-week-old *Fam20a*$^{fl/fl}$ (A) and *Sox2-Cre;Fam20a*$^{fl/fl}$ (B) mice. A1 and B1 are the higher magnification views of the areas marked in black boxes in A and B, respectively. There was no obvious difference in odontoblast morphology between the *Fam20a*$^{fl/fl}$ and *Sox2-Cre;Fam20a*$^{fl/fl}$ mice. C-F, representative immunohistochemical staining results (signal in brown) of DMP1 (C and D) and DSPP (E and F) in the mandibular first molars of 3-week-old *Fam20a*$^{fl/fl}$ (C and E) and *Sox2-Cre;Fam20a*$^{fl/fl}$ (D and F) mice. C1-F1 are the higher magnification views of the areas marked in black boxes in C-F, respectively. G-J, representative *in situ* hybridization (signal in purple) analyses of DMP1 (G and H) and DSPP (I ad J) mRNAs in the mandibular first molars of 3-week-old *Fam20a*$^{fl/fl}$ (G and I) and *Sox2-Cre;Fam20a*$^{fl/fl}$ (H and J) mice. Note that there were no apparent differences in DMP1 and DSPP expression levels in the odontoblasts between the *Fam20a*$^{fl/fl}$ and *Sox2-Cre;Fam20a*$^{fl/fl}$ mice. Abbreviations: od, odontoblast; pd, predentin; and d, dentin. Scale bars: 200 μm in A-J, and 20 μm in A1-F1.

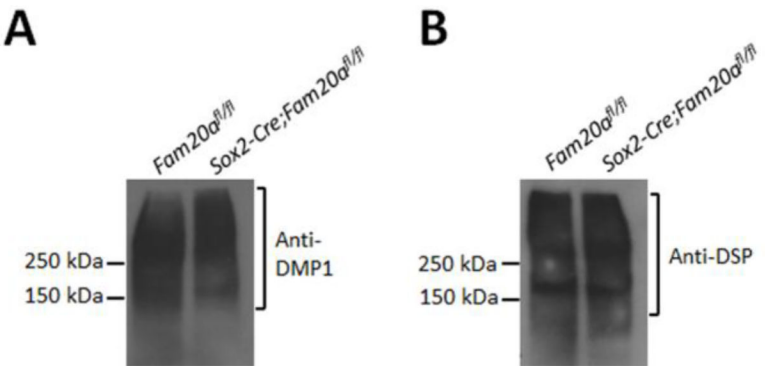

Fig. 8. Western immunoblotting analyses of DMP1 and DSP/DSPP

Western immunoblotting analyses of DMP1 (A) and DSP/DSPP (B) in the total proteins extracted from the first molars of 3-week-old *Fam20a*$^{fl/fl}$ and *Sox2-Cre;Fam20a*$^{fl/fl}$ mice. Note that there was no obvious differences in the levels of DMP1- and DSP/DSPP-related proteins between the *Fam20a*$^{fl/fl}$ and *Sox2-Cre;Fam20a*$^{fl/fl}$ mice.

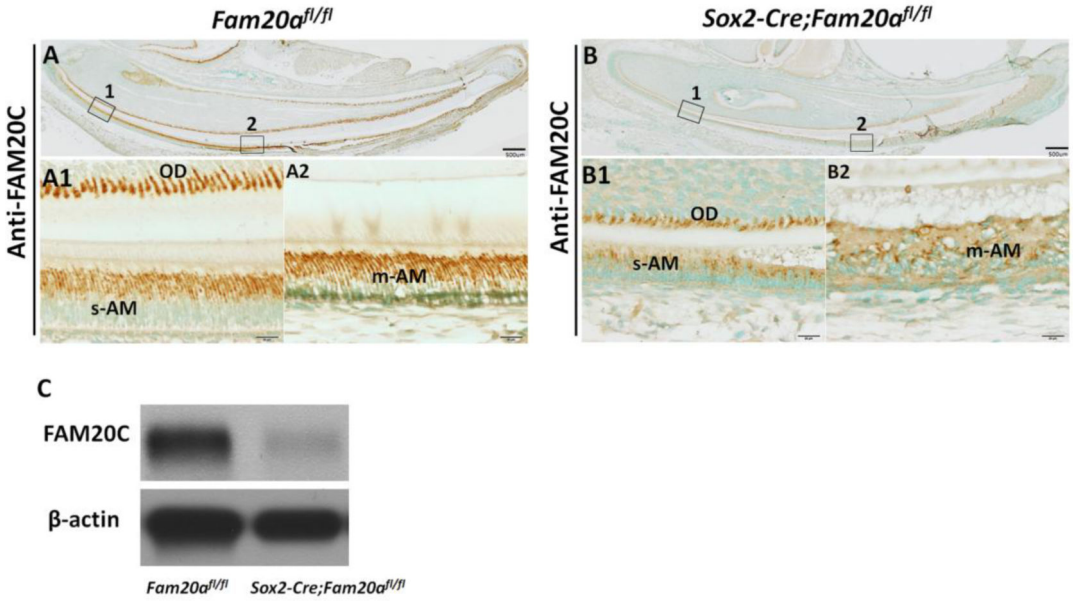

Fig. 9. Reduced FAM20C protein levels in the *Sox2-Cre;Fam20a*$^{fl/fl}$ mice

A and B, representative immunohistochemical results (signal in brown) of FAM20C on the sagittal sections of the mandibular incisors of 7-day-old *Fam20a*$^{fl/fl}$ (A) and *Sox2-Cre;Fam20a*$^{fl/fl}$ mice (B). A1 and B1 are the higher magnification views of the secretory stage ameloblasts in black boxes 1 in A and B, respectively. A2 and B2 are the higher magnification views of the maturation stage ameloblasts in black boxes 2 in A and B, respectively. C. Western immunoblotting analysis of FAM20C in the enamel organs of the mandibular incisors isolated from 3-day-old *Fam20a*$^{fl/fl}$ and *Sox2-Cre;Fam20a*$^{fl/fl}$ mice. Immunohistochemical staining showed that FAM20C was dramatically reduced in both ameloblasts and odontoblasts in the *Sox2-Cre;Fam20a*$^{fl/fl}$ mouse incisors, compared to the *Fam20a*$^{fl/fl}$ mouse incisors. Western immunoblotting analyses confirmed the decreased FAM20C in the *Sox2-Cre;Fam20a*$^{fl/fl}$ mouse incisors, compared to the *Fam20a*$^{fl/fl}$ mouse incisors. Scale bars: 500 μm in A and B; 20 μm in A1, A2, B1 and B2.